Neurobiology of Aging 104 (2021) 1–9

Contents lists available at ScienceDirect

Neurobiology of Aging

journal homepage: www.elsevier.com/locate/neuaging.org

Association between metabolic syndrome and resting-state functional brain connectivity

Barnaly Rashid[a,b,c,*], Victoria N. Poole[a,b], Francesca C. Fortenbaugh[a,b], Michael Esterman[e,a,d], William P. Milberg[a,b], Regina E. McGlinchey[a,b], David H. Salat[a,b,c], Elizabeth C. Leritz[a,b]

[a] Neuroimaging Research for Veterans Center (NeRVe), Geriatric Research Education and Clinical Center (GRECC), VA Boston Healthcare System, Boston, MA, USA
[b] Harvard Medical School, Boston, MA, USA
[c] The Athinoula A. Martinos Center for Biomedical Imaging, Boston, MA, USA
[d] Department of Psychiatry, Boston University School of Medicine, Boston, MA, USA
[e] National Center for PTSD, VA Boston Healthcare System, Boston, MA

ARTICLE INFO

Article history:
Received 15 June 2020
Revised 18 March 2021
Accepted 24 March 2021
Available online 1 April 2021

Keywords:
fMRI
Functional connectivity
Metabolic syndrome
Cardiovascular Health
Vascular risks

ABSTRACT

The objective of this study is to examine whether metabolic syndrome (MetS), the clustering of 3 or more cardiovascular risk factors, disrupts the resting-state functional connectivity (FC) of the large-scale cortical brain networks. Resting-state functional magnetic resonance imaging data were collected from seventy-eight middle-aged and older adults living with and without MetS (27 MetS; 51 non-MetS). FC maps were derived from the time series of intrinsic activity in the large-scale brain networks by correlating the spatially averaged time series with all brain voxels using a whole-brain seed-based FC approach. Participants with MetS showed hyperconnectivity across the core brain regions with evidence of loss of modularity when compared with non-MetS individuals. Furthermore, patterns of higher between-network MetS-related effects were observed across most of the seed regions in both right and left hemispheres. These findings indicate that MetS is associated with altered intrinsic communication across core neural networks and disrupted between-network connections across the brain due to the co-occurring vascular risk factors in MetS.

1. Introduction

Cardiovascular risk factors (RFs), such as hypertension, obesity and higher level of cholesterol, rarely occur in isolation. These RFs often appear in clusters, and the clustering of 3 or more vascular RFs is defined as the metabolic syndrome (MetS) (Grundy, 2005). The overall prevalence of MetS has been alarmingly increasing every year in the middle aged and older adults among the US population as well as nations abroad (Aguilar et al., 2015; Arai et al., 2010; Beltrán-Sánchez et al., 2013; Grundy, 2008; Shin et al., 2018), making it an emerging global health concern. Further, MetS can lead to accelerated brain aging and increased risk for neurodegenerative diseases, including Alzheimer's disease (AD) (Misiak et al., 2012; Raffaitin et al., 2009) and vascular dementia (Panza et al., 2011; Solfrizzi et al., 2011). While the relationships between isolated RFs and neural integrity have been previously examined (Beltrán-Sánchez et al., 2013; Kim and Feldman, 2015; Misiak et al., 2012; Raffaitin et al., 2009; Van den Berg et al., 2007; Yaffe et al., 2004; Yaffe et al., 2009), very little is known about how the shared contribution of RFs in MetS disrupts functional organization and temporal dependency across core brain networks. Moreover, changes in functional brain measures due to MetS may arise before even any measurable structural alterations and cognitive impairment, and therefore, it is critical to examine the MetS-specific effects on brain functions and functional networks. Previously, resting-state functional connectivity (FC) has been used to identify altered communication among brain networks in a range of neurological conditions with vascular origins (Diciotti et al., 2017; Schaefer et al., 2014; Sun et al., 2011), including Alzheimer's disease (Greicius et al., 2004; Sorg et al., 2009), and mild cognitive impairment (Bai et al., 2009). Thus, resting-state FC can offer valuable measures to understand altered neural integrity in the presence of MetS.

Key: mm, millimeter; LH, left hemisphere and RH= right hemisphere.

* Corresponding author at: Barnaly Rashid,VA Boston Healthcare System, 150 S Huntington Ave, Boston, MA 02130, USA. Tel.: 857 364 5645, fax: 857 364 4544.
E-mail address: barnaly_rashid@hms.harvard.edu (B. Rashid).

0197-4580/$ – see front matter © 2021 Elsevier Inc. All rights reserved.
https://doi.org/10.1016/j.neurobiolaging.2021.03.012

MetS and its component RFs have been previously associated with both brain structure (Alfaro et al., 2018; Alfaro et al., 2016; Sala et al., 2014; Schwarz et al., 2018; Yates et al., 2012) and function (Haight et al., 2015; Kenna et al., 2013). However, only few studies have explored the FC measures with regard to MetS or its RFs (Musen et al., 2012; Park et al., 2018; Rashid et al., 2019). Further, associations between specific components of MetS and cognition have been previously well established. For example, the domains of executive function and attention, particularly responsible for higher order cognitive processing, have been associated with higher blood pressure (BP) (Bucur and Madden, 2010; Gorelick and Nyenhuis, 2012), high cholesterol (Leritz et al., 2016; Wendell et al., 2014; Xia et al., 2015b), and diabetes (Vincent and Hall, 2015). These previous findings provide evidence of altered structural and functional neural integrity due to vascular RFs and MetS and support the necessity to further investigate whole-brain FC patterns that might be targeted by MetS. Moreover, since MetS has been reported to disrupt aspects of cognition, including executive function, memory, and attention (Wooten et al., 2019), a whole-brain approach allows us to examine FC networks that may underlie more specific cognitive domains.

In the current study, using a seed-based approach we examined the FC among the core functional networks. We hypothesize that the shared underlying pathophysiological mechanisms of the co-occurring RFs in MetS interrupting neural metabolic health (i.e., cerebrovascular functioning) also disrupt neural integrity in the brain. Further, we hypothesize that individuals with MetS will demonstrate disrupted resting state whole-brain FC, particularly in the between-network FC among higher-order networks associated with attentional and executive control domains, compared to individuals without co-occurring RFs.

2. Methods

2.1. Standard protocol approvals and patient consents

The study was approved and monitored by the Institutional Review Board of the Veterans Administration Boston Healthcare System (VA), Jamaica Plain, MA, USA. All participants provided signed informed consent prior to study procedures.

2.2. Participants

Seventy-eight adults agreeing to undergo structural and functional MRI participated in this study. Twenty-seven were identified with MetS (i.e., 3 or more RFs (Expert Panel on Detection, 2001; Grundy et al., 2005)) (MetS, age (mean ± SD): 65.70 ± 7.87, 3 females) and the remaining 51 comprised the non-MetS group (less than 3 RFs; age (mean ± SD): 59.63 ± 8.60, 19 females).

Table 1 displays group-wise demographics and characteristics of the participants. Individuals were enrolled from direct clinic recruitment in VA Boston clinics to target those at high risk for MetS, as well as through advertisement in the greater Boston, Massachusetts (USA) metropolitan area. Inclusion criteria required participants to be English speakers and between the ages of 30–90. Participants were excluded for the following reasons: a history of head trauma of moderate to severe severity (e.g., loss of consciousness greater than 30 minutes, diagnosis of any form of dementia, past or current history of severe psychiatric illness, history of major surgery (e.g., brain or cardiac), significant neurologic illness, history or current diagnosis of drug abuse or dependence. Exclusion criteria also included any contraindication to magnetic resonance imaging (MRI), such as a pacemaker or other metal implant.

2.3. Risk factor measurement

To assess the RFs, the following measures were collected:

- Fasting blood (12 hr) was drawn and processed for analysis of serum RF levels, including triglycerides, HDL-C and fasting plasma glucose.
- Systolic and diastolic BP were recorded in a seated position after 5 minutes of rest with the arm at rest, at the level of the heart, using a standard sphygmomanometer. A second measurement was obtained 5 minutes later and the average of 2 values was recorded.
- Waist circumference measurement was taken while standing, to the nearest centimeter, with measuring tape placed around the abdomen at the level of the umbilicus.
- Medications taken to treat hypertension, diabetes, or abnormal cholesterol were reported by participants and recorded by an examiner.

2.4. Metabolic syndrome

MetS criteria were determined from the RF measures. Participants with MetS were defined as meeting thresholds (Grundy, 2005) for 3 or more of the following component RFs: (1) elevated waist circumference ≥102/88 cm (male/female); (2) elevated triglycerides ≥150 mg/dL or drug treatment for dyslipidemia; (3) reduced HDL-C <40/50 mg/dL (male/female) or drug treatment for dyslipidemia; (4) elevated systolic BP ≥130 mmHg or diastolic BP ≥85 mmHg or drug treatment for hypertension, and (5) elevated fasting plasma glucose ≥100 mg/dL or drug treatment for elevated glucose or diabetes.

2.5. Imaging data acquisition

For 70 participants, neuroimaging data were acquired on a 3-Tesla Siemens (Erlangen, German Prisma Fit 60 cm bore (RF coil ID) using a transmission body coil and a 32-channel reception head coil.

The first 8 participants were scanned prior to the scanner upgrade, on a 3-Tesla Siemens (Erlangen, Germany) TIM Trio scanner, using a transmission body coil and a 32-channel reception head coil. Two MPRAGE (Magnetization Prepared Rapid Gradient Echo) T1-weighted structural scans (repetition time (TR)/echo time (TE): 2530/3.35 ms, flip angle = 7°, inversion time = 1200 ms, field of view=256 × 256 mm, acquisition matrix 256 × 256, 176 contiguous sagittal slices, voxel size = 1 × 1 × 1 mm) were acquired for surface reconstruction, FC seed placement, and inter-participant registration. Resting state functional data were acquired in a single run (gradient echo echo-planar imaging, TR/TE: 4000/31 ms, flip angle: 90°, field of view =128 × 128 mm, voxel size 2 × 2 × 2.5 mm, 55 axial slices, 90 volumes, 6:12 min per run). Prior to scanning, participants were instructed to keep their eyes open and stay awake.

2.6. fMRI data preprocessing

A model of each subject's cortical surface was reconstructed from the T1 -weighted MRI volume using FreeSurfer, as described previously (Dale et al., 1999; Lindemer et al., 2013). Functional neuroimaging data were processed using a combination of FreeSurfer (Fischl et al., 1999), AFNI (Cox, 1996), and FSL (Jenkinson et al., 2012) based on the FSFAST processing stream (http://freesurfer.net/fswiki/FsFast). Resting state functional magnetic resonance imaging (fMRI) data were preprocessed using a standard stream (i.e., motion correction using 6 parameters, time

Table 1
Group-wise demographic data and risk factors

	Non-MetS (N = 51)	MetS (N = 27)	Significance tests
Age (years)	59.63 ± 8.60	65.70 ± 7.87	Student's $t(76) = -3.06$, $p = 0.003$*
Sex (female/male)	19/32	3/24	Fisher's exact test: $p = 0.018$*
Waist circumference (cm)	89.72 ± 13.90	105.26 ± 15.92	Student's $t(76) = -4.47$, $p = 2.72e\text{-}05$**
Triglycerides (mg/dL)	91.21 ± 47.48	105.70 ± 43.96	Welch's $t(56.77) = -1.34$, $p = 0.183$
HDL-C (mg/dL)	61.92 ± 17.04	51.04 ± 14.84	Student's $t(76) = 2.80$, $p = 0.006$*
Systolic BP (mm Hg)	122.37 ± 17.59	131.52 ± 14.71	Student's $t(76) = -2.31$, $p = 0.024$*
Diastolic BP (mm Hg)	72.94 ± 11.15	76.19 ± 8.34	Student's $t(76) = -1.33$, $p = 0.189$
Fasting blood glucose (mg/dL)	91.90 ± 14.66	104.59 ± 14.42	Welch's $t(53.86) = -3.68$, $p = 0.0005$**
Cardiovascular/Diabetes Medication			
Blood Pressure (N (%))	7 (13.73 %)	18 (66.67%)	Fisher's exact test: p value = 4.876e-06**
Glucose(N (%))	1 (1.96%)	5 (18.52%)	Fisher's exact test: p value = 0.017*
Triglycerides (N (%))	1 (1.96%)	16 (59.26%)	Fisher's exact test: p value = 1.074e-08**
Risk Factor Criteria			
Met Waist Circumference (N (%))	12 (23.53%)	19 (70.37%)	Fisher's exact test: p value = 8.577e-05**
Met Triglycerides (N (%))	3 (5.88%)	21 (77.78%)	Fisher's exact test: p value = 7.928e-11**
Met HDL-C (N (%))	4 (7.84%)	8 (29.63%)	Fisher's exact test: p value = 0.019*
Met BP (N (%))	18 (35.29%)	26 (96.29%)	Fisher's exact test: p value = 5.59e-08**
Met Glucose (N (%))	5 (9.80%)	22 (81.48%)	Fisher's exact test: p value = 2.895e-10**

Continuous variables are presented as mean ± standard deviation. Group-wise number of participants on cardiovascular medications is presented. Also, group-wise number of participants meeting each of the risk factors' criterion is reported.
Key: cm, centimeter; mg/dL, milligrams per deciliter; HDL-C, high-density lipoprotein cholesterol; mm Hg, millimeters of mercury.
* $p < 0.05$
** $p < 0.001$

shifting, concatenation of scans, motion regressed from time series, regression of the global mean and the average time course from the white matter and ventricles, band pass filtering between 0.01 and 0.1 Hz). Time points and participants with excessive motion were excluded (0.5 mm/TR; 20 TRs/participant; Figure S9). Additional validations for motion artifact are provided in Figure S8. Data were sampled to and smoothed on the surface, and each brain was warped to a surface-based template (fsaverage) (Fischl et al., 1999).

The 7-network surface-based functional parcellation published by Yeo et al. (Thomas Yeo et al., 2011) were used to extract individual cluster time series associated with default-mode network (DMN), dorsal attention network (DAN), executive control network (ECN), visual network (VIS), sensorimotor network (SM), ventral attention network (VAN) and limbic network (LIMBIC). The spatially averaged time series of each of these 7 regions served as seeds for whole-brain voxel-wise correlation (FC) maps in each individual. Group level analyses are described below.

2.7. Statistical analyses

Group differences in age, waist circumference, triglycerides, HDL-C, systolic and diastolic BP, and fasting blood glucose were examined either with independent two-sample Student's t tests (for normally distributed data as assessed with a Shapiro-Wilk test), the Wilcoxon rank-sum test with continuity correction (for non-normally distributed data), or the Welch's t test (when there was a significant group difference in variance as assessed with an F-test). To examine group differences on categorical variables such as gender, Fisher's exact test was employed. Statistical analyses were two tailed with an alpha level set at $p < 0.05$ and carried out in R (Version 3.2.2). Table 1 presents the group difference in demographic data.

Group differences and associations (see Table 2) were computed at each vertex over the cortex using multiple linear regression using FreeSurfer's mri_glmfit function, and custom scripts in MATLAB (Mathworks; Natick, MA). The nuisance regressors of age, sex and scanner were included in all models unless otherwise noted. Family-wise corrections for multiple comparisons were simulated with pre-computed Monte-Carlo simulations of 10,000 iterations using FreeSurfer's mri_glmfit-sim function, with vertex- and cluster-wise thresholds of $p < 0.05$. Fig. 1, Figure S2 and Figure S3 highlight the group differences in FC. Effects of age (Figure S4 and Figure S5), sex (Figure S7), scanner (Figure S10) and white matter hypointensities (Figure S6) on FC were evaluated.

2.8. Within- and between- network FC effects

In addition to group differences in network connectivity maps, within- and between-seed FC measures were estimated as shown in Fig. 2. For a particular difference map, the following steps were followed to estimate within- and between-network FC:

- Within-network effects were computed as the total count of vertices belonging to the same network seed region. For example, from the group difference in FC when using the DMN seed, the vertices that belong to the DMN region were considered as within-DMN FC effects.
- Between-network effects were computed as the count of vertices belonging to regions outside of the network seed. For example, from the group difference in FC when using the DMN seed, the vertices that belong to all other regions but the DMN were considered as between-DMN FC effects.
- Finally, the percentage of within- and between-seed FC effects were computed relative to the total count of vertices within the seed (network) region.

Figure S1 provides more details on the estimation of within- and between-network FC effects.

2.9. Data availability statement

The data that support the findings of this study are available on request from Dr. Elizabeth C. Leritz. The data are not publicly available due to privacy or ethical restrictions (funding agency: National Institute of Neurological Disorders and Stroke, grant number: NS086882, PI: Elizabeth C. Leritz, study title: Neuroimaging and neuropsychological biomarkers of vascular RFs).

Table 2
Summary information on clusters that survived multiple comparison correction in general linear model (GLM) analysis

Network	Hemisphere	Significant cluster	Number of vertices	Cluster size (mm^2)	Maximum t-value	MNI (x, y, z)
Default-mode	LH	DMN	11002	5310.40	-3.66	-45.6, 21.6, 7.9
Network (DMN)	RH	SM	9032	3844.70	-3.69	57.8, -3.3, -8.3
	RH	ECN	8164	4346.61	-3.16	41.8, 24.8, 20.9
Dorsal Attention	LH	VIS	11480	33763	-4.74	-19.9, -71.4, 18.2
Network (DAN)	RH	DMN	4013	2049.82	3.84	52.4, 8.6, -17.8
	RH	VIS	12100	7784.91	-3.83	20.7, -71.8, 20.2
Executive Control	RH	VAN	8390	3807.12	-5.13	48.9, -2.7, 9.0
Network (ECN)	RH	SM	15098	6275.46	-4.11	6.1, -3.4, 40.6
Visual Network	LH	DAN	8065	4763.88	-3.25	-51.3, -41.6, -25
(VIS)	RH	LIMBIC	3287	1956.04	-3.59	45.3, -11.5, -37.4
Sensori-motor	LH	DAN	12943	5711.36	-4.84	-25.6, -57.8, 45.9
Network	LH	DAN	7699	4494.11	-4.49	-21.0, 4.4, 49.4
(SM)	RH	DAN	3839	1692.50	-3.53	26.7, -59.8, 46.6
Ventral Attention	LH	DMN	4711	2807.71	-4.27	-9.2, 59.7, 7.3
Network (VAN)	LH	VIS	6715	3193.33	-2.99	-20.4, -61.6, 13.6
	RH	DMN	6181	3467.27	-4.02	8.2, 31.1, 11.7
Limbic Network	RH	LIMBIC	2335	1749.70	3.45	26.2, 58.2, -10.5
(LIMBIC)						

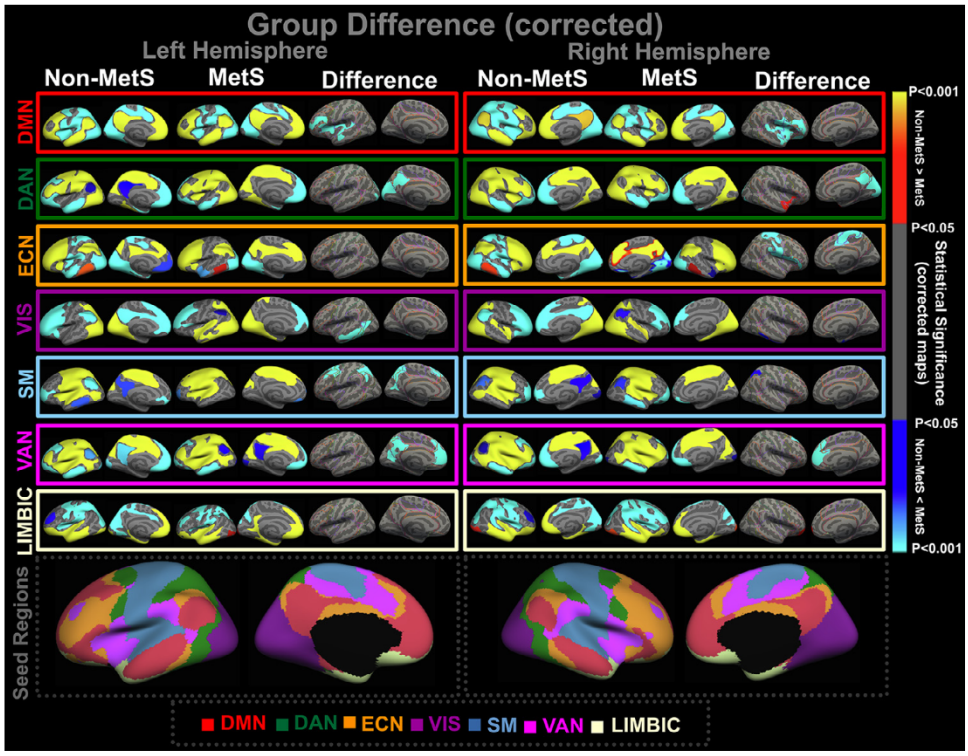

Fig. 1. Group difference in functional connectivity (FC). One-sample group mean (OSGM) results from FC analyses for non-metabolic syndrome (Non-MetS, N = 51; risk factors ranging from 0–2) and patients with metabolic syndrome (MetS, N = 27; 3 or more risk factors), and their group differences in brain network FC after corrected for multiple comparisons ($p < 0.05$). Uncorrected maps of the group differences in network FC are provided in supplemental Figure S2. Composite maps of group difference are presented in supplemental Figure S3 summarizing the group difference across all 7 functional networks, and are color-coded based on the underlying seed regions. Results are corrected for age and sex. DMN: default-mode network; DAN: dorsal attention network; ECN: executive control network; VIS: visual network; SM: sensorimotor network; VAN: ventral attention network; LIMBIC: limbic network. The color bar indicating "red to yellow: non-MetS > MetS"; and "blue to cyan: MetS > non-MetS".

3. Results

3.1. Demographics and risk factors

The MetS group was significantly older ($p = 0.003$) and had a larger proportion of males ($p = 0.018$) relative the HC group (Table 1).

Further, significant group difference in waist circumference ($p = 2.72e\text{-}05$), HDL-C ($p = 0.006$), systolic ($p = 0.024$) BP, and fasting blood glucose ($p = 0.0005$) were observed. No significant group differences were observed in triglycerides ($p = 0.183$) and diastolic BP ($p = 0.189$).

3.2. Group difference in functional connectivity

For each seed and for each hemisphere, Fig. 1 presents the corrected (multiple comparisons test at $p < 0.05$) FC results from the GLM analysis showing the (1) one-sample group mean measures of FC in non-MetS and MetS groups, and (2) the group differences in FC of the seed to the rest of the brain regions, after regressing out scanner-, age- and sex-effects. The composite regions of interest (ROI) maps (Figure S3) provide an overview of how much significant group–related effects were found across each hemisphere (i.e., effects are color-coded based on the underlying seed regions).

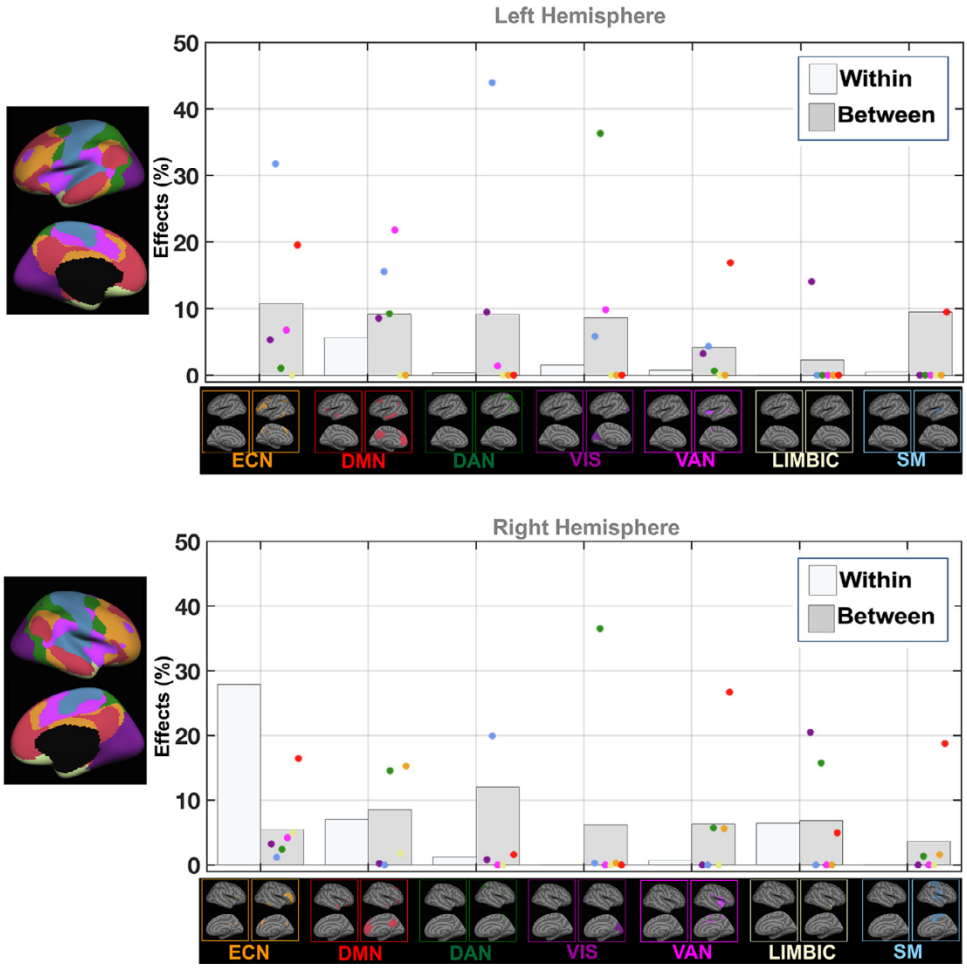

Fig. 2. Within- and between-network effects of mets. Bar plots showing MetS-related significant within- and between-network associations (%) in functional connectivity (FC) across brain networks. Each dot is colored based on the associated seed region for a specific network (e.g., red dot = default mode network), and represents the association between MetS and the disrupted FC between a particular seed region and that network. DMN, default-mode network; DAN, dorsal attention network; ECN, executive control network; VIS, visual network; SM, sensorimotor network; VAN, ventral attention network; LIMBIC, limbic network. Supplementary Figure S1 provides the details on estimation the within- and between-network association measures.

Table 2 provides the number of vertices, cluster size (in mm^2) maximum t-value and MNI coordinates for each of the significant clusters showing network-level group effect in right and left hemispheres.

3.2.1 Default. mode network (DMN)

Relative to the non-MetS group, the MetS group demonstrated significantly greater within-DMN FC, and FC between DMN and ECN, VAN and SM regions in the left hemisphere. In the right hemisphere, the MetS group showed significantly greater within-DMN FC, and FC between DMN and ECN, DAN, VAN, LIMBIC and SM regions.

3.2.2. Dorsal attention network (DAN)

The MetS group demonstrated significantly greater within-DAN FC in both hemispheres. In the left hemisphere, compared to the non-MetS group, the FC measures between DAN and ECN, DMN and VAN regions were greater for the MetS group, whereas in the right hemisphere, the FC measures between DAN and ECN, DMN, VAN, LIMBIC and SM regions were greater for the MetS group.

3.2.3. Executive control network (ECN)

No within-ECN group difference in FC was observed in the left hemisphere, whereas in the right hemisphere, the MetS group exhibited significantly greater within-ECN FC compared to the non-MetS group. No group difference in FC was found between ECN and any other regions in the left hemisphere. In the right hemisphere, relative to the non-MetS group, the MetS group showed significantly greater FC between ECN and DMN, VAN and SM regions.

3.2.4. Visual network (VIS)

The MetS group exhibited greater within-VIS FC in the left hemisphere, while no group difference in within-VIS FC was highlighted in the right hemisphere. For between-network, compared to the non-MetS group, significantly greater FC measures between VIS and ECN, DMN, DAN, VAN and LIMBIC regions were captured in the left hemisphere, and significantly greater FC measures between VIS and ECN, DAN, VAN and LIMBIC regions were observed in the right hemisphere in the MetS group.

3.2.5. Sensorimotor network (SM)

In the left hemisphere, relative to non-MetS, the MetS group exhibited significantly greater within-SM FC, and FC between SM and ECN, DMN, DAN, VIS and VAN regions. In the right hemisphere, no group difference was found for within-SM FC measures, and relative to non-MetS, the MetS group exhibited significantly greater FC between SM and ECN and DAN regions.

3.2.6. Ventral attention network (VAN)

In both hemispheres, within-VAN FC measures were significantly greater in the MetS group. The FC measures between VAN and ECN, DMN, DAN and VIS regions were significantly greater in the left hemisphere, and the FC between VAN and ECN was significantly greater in the right hemisphere within the MetS group compared to the non-MetS group.

3.2.7. Limbic network (LIMBIC)

No significant clusters exhibiting group differences were identified in the left hemisphere. For the right hemisphere, the within-LIMBIC FC was greater in the non-MetS group, and the FC measures between LIMBIC and ECN and DMN regions were greater in the non-MetS group.

3.3. Within- and between-network effects

Fig. 2 illustrates the within- and between-network effects for each hemisphere. Except for few seed regions, most between-network effects were observed across both hemispheres. In the left hemisphere, the ECN, DMN, DAN and VIS seed regions showed higher between-seed effects, ranging from 8.7-10.8%, with only DMN exhibiting relatively greater within-DMN effects (5.6%) compared to other brain networks. Interestingly, in the right hemisphere, the ECN seed showed greater within-ECN effect (27.9%), and the DMN seed showed similar within-DMN (7%) and between-DMN (8.5%) effects. The LIMBIC seed also showed similar within-LIMBIC (6.4%) and between-LIMBIC (6.8%) effects in the right hemisphere. Other seed regions showed consistent patterns of relatively higher between-seed effects in the right hemisphere.

4. Discussion

The current study investigates the associations between MetS and resting-state whole-brain FC measures across core networks. The main findings reveal that: (1) patients with MetS exhibit hyperconnectivity across several brain networks, including those supporting higher-order cognitive functions (i.e., DMN, ECN, DAN and VAN), when compared with non-MetS individuals; and (2) MetS more prominently affected inter-network communication (i.e., between-networks) than intra-network communication. These findings suggest that the clustering of vascular RFs in individuals with MetS is associated with the disrupted specialization (and functional independence) of core brain networks underlying attention and executive control.

Our findings of altered hyperconnectivity in individuals with MetS are consistent with previous studies demonstrating altered FC in the context of 1 or more of these component RFs. For example, in a recent study focusing on patients with diabetes, Cui et al. reported reduced DMN connectivity, which was also associated with worse performance on tasks of memory and executive functioning (Cui et al., 2015). Further, in a multimodal structural-functional connectivity study, Park et al. found disrupted frontoparietal network FC based on degree centrality values from individuals with abdominal obesity (Park et al., 2018). In patients with MetS, Rashid et al. identified disrupted FC among the DMN and several brain regions (e.g., superior frontal, superior parietal and postcentral regions) (Rashid et al., 2019). Another study (Xia et al., 2015a) determined associations between Type 2 diabetes mellitus and reduced attentional state across the domains of DAN and VAN. Further, Cui et al. identified association between occipital hypoconnectivity and impaired visual memory and executive function performance in patients with diabetes (Cui et al., 2016). Using graph-theoretical analysis, Baek et al. found altered network topological structures in obesity in both whole-brain network and regional levels (Baek et al., 2017). However, except Rashid et al. (2019), these studies did not specifically investigate MetS, and therefore did not determine the aggregate RFs associations. Here, we demonstrate that multiple co-occurring vascular RFs may be associated with disrupted core brain networks, particularly in DMN, ECN and dorsal/ventral attentional regions. This is critical, as it demonstrates that it is likely the comorbidity of RFs in MetS that associates with these disrupted FC patterns, beyond the individual RF association. Given the fact that most RFs do not occur in isolation, our results provide important evidence of the underlying whole-brain functional network disruption that we believe is specific to MetS.

Our findings reinforce the prior evidence at the whole-brain connectivity level, by demonstrating that the higher-order brain networks that are vital to everyday functional ability, including DMN, DAN and ECN, have altered interactions among themselves due to the co-occurring RFs in MetS. Previously, the domains of executive function and attention, particularly responsible for higher order cognitive processing (e.g., reasoning, planning and cognitive flexibility), has been associated with isolated vascular RFs (Bucur and Madden, 2010; Gorelick and Nyenhuis, 2012; Leritz et al., 2016; Vincent and Hall, 2015; Wendell et al., 2014; Xia et al., 2015b). Our results show that the FC measures across the DMN, DAN, VIS and SM networks are disrupted more globally in the MetS group (i.e., the patterns of FC alteration for these networks are associated with the majority of other core brain networks), whereas the FC measures across the ECN, VAN and LIMBIC networks exhibit more localized alteration patterns in the MetS group (i.e., the patterns of FC alteration for these networks are associated with specific core brain networks). These observed findings of altered FC across the cognitive networks further support prior studies of vascular RFs and cognition. For example, a recent paper from our lab reported a significant effect of vascular RFs on sustained attention whereby better performance was associated with fewer RFs (Wooten et al., 2019). Moreover, our findings indicate that comorbid RFs in MetS might associate with disruption in between-network FC patterns more than the within-network connectivity, which might be due to MetS-associated alterations in underlying brain structure. Indeed, this novel finding is supported by a recent study that reported a significant decrease in between-network fibers in participants with cardiovascular RFs, and suggested that this loss of between-network fibers might reduce their overall network efficiency by disrupting the underlying topological organization (Marebwa et al., 2018).

One interesting observation is that the increases in between-network connectivity (i.e., hyperconnectivity) relative to non-MetS reflect a *decrease in decoupling* (i.e., anti-correlation) across functionally distinct neural networks. This suggests that MetS introduces failures of distinction, perhaps by coherence via altered cerebral hemodynamics or by damage to specific brain regions. For example, when examining DMN connectivity in this larger subset, we observed notable spatial patterns across both hemispheres. The DMN, which is typically decoupled (i.e., anti-correlated) with other networks during extrinsic goal-directed tasks, was no longer decoupled with regions at an intersection of networks spanning the insula, superior temporal, and inferior frontal lobes. Interestingly, this cluster of regions is also supplied by superior and inferior branches of the middle cerebral artery (Birdsill et al., 2013). Per our hypothesis, it is likely that if these regions endure poor perfusion, they may be at a collective risk for increased rate of atrophy, white matter structural damage, and poor function (Liu et al., 2018).

Brain laterality has been previously identified as an important disease characteristic across several brain disorders as well as with normative aging. For instance, prior findings have reported significant left lateralized cortical thinning in the medial temporal region

in patients with AD (Singh et al., 2006). Further, DMN resting-state FC was found to be more left lateralized in patients progressing to AD (Banks et al., 2018). Another study highlighted lateralization of both hypo- and hyper-connectivity in patients with carotid stenosis (Huang et al., 2018). Further, abnormal lateralization in FC has been reported in autism spectrum disorder, a neurodevelopmental disorder, where significantly reduced left lateralization in regions associated with language regions and DMN regions was observed (Nielsen et al., 2014). Other prior findings include aberrant lateralization in froontotemporal dementia (Guo et al., 2016), and effects of aging in brain lateralization (Reuter-Lorenz et al., 2000). Our current findings also show patterns of lateralization in altered FC in the MetS group, for example, more left lateralized FC in the ECN and VAN networks, and right lateralized FC in the LIMBIC network. These findings show great potential for more specific MetS-related associations with altered FC measures, although additional quantitative estimation of lateralization is required before using these findings as robust biomarkers for MetS.

Evidence for region-specific damage in the posterior cerebral artery also exists. For example, MetS related damage to the posterior cingulate cortex, the DMN hub, would account for the altered inter-network communication with the DAN and VAN observed in Fig. 1. Other patterns were apparent in ECN, SM, and DAN group connectivity maps, where MetS related anti-correlations were weakened in network-adjacent regions. Overall, these findings point to non-specific, but widespread, patterns of decoupling across higher-order networks in MetS.

Our study provides evidence of functional significance of the comorbid RFs in MetS with regard to core brain networks associated with critical brain functions, such as executive function and attention, and can be valuable from a clinical standpoint. Conditions such as diabetes, high BP and even MetS are vastly underrepresented in the literature, despite having high prevalence in the aging population, suggesting that there is a lack of clinical confirmation for these diseases. Our findings can provide additional support to clinical interpretation, although more robust and rigorous FC biomarker identification is warranted.

4.1. Limitations

Several experimental and methodological limitations must be considered while interpreting the results of this study.

4.1.1. Sample size

First, relative to the non-MetS group, the number of participants in MetS group is considerably lower, with overall only few female participants. Inclusion of more MetS participants would increase the robustness and the power of the analyses.

4.1.2. Impact of white matter lesions on brain connectivity

While our analyses (Figure S6) revealed no significant associations between white matter lesions (i.e., white matter hypointensities) and significant FC clusters (i.e., ROIs), it is expected that there would be some impact of white matter lesions on the overall seed regions' connectivity, which might explain the laterality effects across our findings.

4.1.3. Impact of motion artifacts on brain connectivity

In this study, we have included the motion-related nuisance variables as regressors during pre-processing. Additionally, in our original analysis, we censored out any TR with greater than 0.5 mm framewise displacement (FD) and removed any participant with censoring of more than 20 TRs (resulted in the removal of 2 MetS participants from our original analyses). However, note that, even with these strict motion removal approaches, it is unlikely to complete remove the motion-related confounds from the MRI data. Therefore, future studies should consider additional validation (for example: Figure S8) to eliminate the possibility of the outcomes to be driven by motion artifacts.

4.1.4. Estimation of distance measures to quantify longer-range connections

In this study, we have utilized the entire network's time series as a "seed". While this provides a broader understanding of network connectivity, it eliminates any within-network diversity that may reveal additional information about disease mechanisms. Further, our "whole network" approach highlights areas of a network that exhibit group differences with the 'mean functional activity' of an entire network, which may significantly skew which areas of the brain gets highlighted. For example, regions that belong to the somato-sensory networks typically exhibit more segregated FC (Chan et al., 2014) or belong to areas less likely to be connector hubs (Bertolero et al., 2015), tend to exhibit lower between-network connectivity; and in cases where sensory-motor areas are connected with another network, it is more likely that they are connected to specific areas of another network. To address this possibility, future work should consider separating a specific functional network into separate but meaningful nodes to explore more precise effects on both within-network and between-network connectivity of higher-order cognitive networks.

4.1.5. Acquisition of multiple runs and longer scan duration

The current study utilized a single run of 6:12 minutes of resting state data. This might limit the ability to use individual-level resting state data and perform 'test-retest' type analysis. Future studies should consider collecting multiple runs and longer scan duration. Also, there was a scanner upgrade during the sample collection, although no significant difference between scanners were observed in mean FC.

4.1.6. Reconciliation of current findings with the existing literature

The current findings show increased within-network connectivity in the MetS group, although studies have previously reported decreased FC in the DMN in patients with vascular RFs (e.g., [1] (Cui et al., 2015), type 2 diabetes; [2] (Beyer et al., 2017), body mass index or BMI ([3] (Musen et al., 2012), type 2 diabetes).Note that, differences in experimental design and methodology can potentially introduce difference in effect directions. For instance, selection of the seed regions/ROIs (e.g., based on the atlas space versus data driven approach, such as independent component analysis or ICA) could introduce variability across the findings. Further, results identified from patients with individual RFs (e.g., diabetes, BP etc.) may vary from results obtained from patients with multiple co-occurring RFs or "metabolic load".

4.1.7. Interpretation of current findings

The current study examined correlational analyses, and therefore inference of causation must be avoided while interpreting the findings. Moreover, for the seed-based approach, each network provides its own overall network strength (in contrary to the conventional within-network nodal strength; see section 4.1.4) and then the relationships among these networks are evaluated. Therefore, some specific within-network attributes (e.g., 'within-network homogeneity', 'within-network variability', or 'within-network connectivity') might not be fully understood. Future studies should investigate nodal-level seeds within a specific network in order to identify these within-network attributes more comprehensively.

5. Summary and conclusion

In summary, MetS is associated with disrupted FC within and between core brain networks, including the DMN, ECN and attention (i.e., DAN and VAN) networks. Moreover, the effects of MetS are more prominent across the between-network FC measures. Future directions will explore how these findings relate to neuropsychological performance.

Authors' contribution

Authors E.C.L and D.H.S. designed the study and wrote the protocol. Author B.R undertook the statistical analysis and wrote the first draft of the manuscript. Authors V.N.P., F.C.F., and M.E. assisted with statistical analysis and manuscript organization. All authors contributed to and have approved the final manuscript.

Disclosure statement

The authors declare no competing financial interests or conflict of interests in relation to the work presented.

Acknowledgements

This work was supported by the National Institute of Neurologic Disorders and Stroke (R01NS), by the National Institute for Nursing Research (R0NR01827), and by the US Department of Veterans Affairs, VA Rehabilitation Research & Development Traumatic Brain Injury Center of Excellence (B9254C). Also, this work was supported by the US Department of Veteran Affairs through a Clinical Science Research & Development Career Development Award (grant number 1IK2CX000706-01A2) to M.E, and a Career Development award from the Department of Veterans Affairs Rehabilitation Research & Development (1IK2RX002268-01A2) to F.C.F.

Supplementary materials

Supplementary material associated with this article can be found, in the online version, at doi:10.1016/j.neurobiolaging.2021.03.012.

References

Aguilar, M., Bhuket, T., Torres, S., Liu, B., Wong, R.J., 2015. Prevalence of the metabolic syndrome in the United States, 2003-2012. JAMA 313 (19), 1973–1974.
Alfaro, F.J., Gavrieli, A., Saade-Lemus, P., Lioutas, V.-A., Upadhyay, J., Novak, V., 2018. White matter microstructure and cognitive decline in metabolic syndrome: a review of diffusion tensor imaging. Metabolism 78, 52–68.
Alfaro, F.J., Lioutas, V.-A., Pimentel, D.A., Chung, C.-C., Bedoya, F., Yoo, W.-K., Novak, V., 2016. Cognitive decline in metabolic syndrome is linked to microstructural white matter abnormalities. J. Neurol. 263 (12), 2505–2514.
Arai, H., Yamamoto, A., Matsuzawa, Y., Saito, Y., Yamada, N., Oikawa, S., Mabuchi, H., Teramoto, T., Sasaki, J., Nakaya, N., 2010. Prevalence of the metabolic syndrome in elderly and middle-aged Japanese. J. Clin. Gerontol. Geriatr. 1 (2), 42–47.
Baek, K., Morris, L.S., Kundu, P., Voon, V., 2017. Disrupted resting-state brain network properties in obesity: decreased global and putaminal cortico-striatal network efficiency. Psychol. Med. 47 (4), 585–596.
Bai, F., Watson, D.R., Yu, H., Shi, Y., Yuan, Y., Zhang, Z., 2009. Abnormal resting-state functional connectivity of posterior cingulate cortex in amnestic type mild cognitive impairment. Brain Res. 1302, 167–174.
Banks, S.J., Zhuang, X., Bayram, E., Bird, C., Cordes, D., Caldwell, J.Z., Cummings, J.L., Initiative, A.s.D.N., 2018. Default mode network lateralization and memory in healthy aging and Alzheimer's disease. J. Alzheimers Dis. 66 (3), 1223–1234.
Beltrán-Sánchez, H., Harhay, M.O., Harhay, M.M., McElligott, S., 2013. Prevalence and trends of metabolic syndrome in the adult US population, 1999–2010. J. Am. Coll. Cardiol. 62 (8), 697–703.
Bertolero, M.A., Yeo, B.T., D'Esposito, M., 2015. The modular and integrative functional architecture of the human brain. Proc. Natl. Acad. Sci. 112 (49), E6798–E6807.
Beyer, F., Kharabian Masouleh, S., Huntenburg, J.M., Lampe, L., Luck, T., Riedel-Heller, S.G., Loeffler, M., Schroeter, M.L., Stumvoll, M., Villringer, A., 2017. Higher body mass index is associated with reduced posterior default mode connectivity in older adults. Hum. Brain Mapp. 38 (7), 3502–3515.
Birdsill, A.C., Carlsson, C.M., Willette, A.A., Okonkwo, O.C., Johnson, S.C., Xu, G., Oh, J.M., Gallagher, C.L., Koscik, R.L., Jonaitis, E.M., 2013. Low cerebral blood flow is associated with lower memory function in metabolic syndrome. Obesity 21 (7), 1313–1320.
Bucur, B., Madden, D.J., 2010. Effects of adult age and blood pressure on executive function and speed of processing. Exp. Aging Res. 36 (2), 153–168.
Chan, M.Y., Park, D.C., Savalia, N.K., Petersen, S.E., Wig, G.S., 2014. Decreased segregation of brain systems across the healthy adult lifespan. Proc. Natl. Acad. Sci. 111 (46), E4997–E5006.
Cox, R.W., 1996. AFNI: software for analysis and visualization of functional magnetic resonance neuroimages. Comput. Biomed. Res. 29 (3), 162–173.
Cui, Y., Jiao, Y., Chen, H.-J., Ding, J., Luo, B., Peng, C.-Y., Ju, S.-H., Teng, G.-J., 2015. Aberrant functional connectivity of default-mode network in type 2 diabetes patients. Eur. Radiol. 25 (11), 3238–3246.
Cui, Y., Li, S.-F., Gu, H., Hu, Y.-Z., Liang, X., Lu, C.-Q., Cai, Y., Wang, C.-X., Yang, Y., Teng, G.-J., 2016. Disrupted brain connectivity patterns in patients with type 2 diabetes. Am. J. Neuroradiol. 37 (11), 2115–2122.
Dale, A.M., Fischl, B., Sereno, M.I., 1999. Cortical surface-based analysis: I. Segmentation and surface reconstruction. Neuroimage 9 (2), 179–194.
Diciotti, S., Orsolini, S., Salvadori, E., Giorgio, A., Toschi, N., Ciulli, S., Ginestroni, A., Poggesi, A., De Stefano, N., Pantoni, L., 2017. Resting state fMRI regional homogeneity correlates with cognition measures in subcortical vascular cognitive impairment. J. Neurol. Sci. 373, 1–6.
Expert Panel on Detection, E., 2001. Executive summary of the third report of the National Cholesterol Education Program (NCEP) expert panel on detection, evaluation, and treatment of high blood cholesterol in adults (Adult Treatment Panel III). JAMA 285 (19), 2486.
Fischl, B., Sereno, M.I., Dale, A.M., 1999. Cortical surface-based analysis: II: inflation, flattening, and a surface-based coordinate system. Neuroimage 9 (2), 195–207.
Gorelick, P.B., Nyenhuis, D., 2012. Blood pressure and treatment of persons with hypertension as it relates to cognitive outcomes including executive function. J. Am. Soc. Hypertens. 6 (5), 309–315.
Greicius, M.D., Srivastava, G., Reiss, A.L., Menon, V., 2004. Default-mode network activity distinguishes Alzheimer's disease from healthy aging: evidence from functional MRI. Proc. Natl. Acad. Sci. 101 (13), 4637–4642.
Grundy, S.M., 2005. Metabolic syndrome scientific statement by the American Heart Association and the National Heart, Lung, and Blood Institute. Am Heart Assoc 25 (11), 2243–2244.
Grundy, S.M., 2008. Metabolic syndrome pandemic. Arterioscler. Thromb. Vasc. Biol. 28 (4), 629–636.
Grundy, S.M., Cleeman, J.I., Daniels, S.R., Donato, K.A., Eckel, R.H., Franklin, B.A., Gordon, D.J., Krauss, R.M., Savage, P.J., Smith Jr., S.C., 2005. Diagnosis and management of the metabolic syndrome: an American Heart Association/National Heart, Lung, and Blood Institute scientific statement. Circulation 112 (17), 2735–2752.
Guo, C.C., Sturm, V.E., Zhou, J., Gennatas, E.D., Trujillo, A.J., Hua, A.Y., Crawford, R., Stables, L., Kramer, J.H., Rankin, K., 2016. Dominant hemisphere lateralization of cortical parasympathetic control as revealed by frontotemporal dementia. Proc. Natl. Acad. Sci. 113 (17), E2430–E2439.
Haight, T.J., Bryan, R.N., Erus, G., Davatzikos, C., Jacobs, D.R., D'Esposito, M., Lewis, C.E., Launer, L.J., 2015. Vascular risk factors, cerebrovascular reactivity, and the default-mode brain network. Neuroimage 115, 7–16.
Huang, K.-L., Chang, T.-Y., Ho, M.-Y., Chen, W.-H., Yeh, M.-Y., Chang, Y.-J., Wong, H.-F., Chang, C.-H., Liu, C.-H., Lee, T.-H., 2018. The correlation of asymmetrical functional connectivity with cognition and reperfusion in carotid stenosis patients. Neuroimage 20, 476–484.
Jenkinson, M., Beckmann, C.F., Behrens, T.E., Woolrich, M.W., Smith, S.M., 2012. Fsl. Neuroimage 62 (2), 782–790.
Kenna, H., Hoeft, F., Kelley, R., Wroolie, T., DeMuth, B., Reiss, A., Rasgon, N., 2013. Fasting plasma insulin and the default mode network in women at risk for Alzheimer's disease. Neurobiol. Aging 34 (3), 641–649.
Kim, B., Feldman, E.L., 2015. Insulin resistance as a key link for the increased risk of cognitive impairment in the metabolic syndrome. Exp. Mol. Med. 47 (3), e149.
Leritz, E.C., McGlinchey, R.E., Salat, D.H., Milberg, W.P., 2016. Elevated levels of serum cholesterol are associated with better performance on tasks of episodic memory. Metab. Brain Dis. 31 (2), 465–473.
Lindemer, E.R., Salat, D.H., Leritz, E.C., McGlinchey, R.E., Milberg, W.P., 2013. Reduced cortical thickness with increased lifetime burden of PTSD in OEF/OIF veterans and the impact of comorbid TBI. Neuroimage 2, 601–611.
Liu, M., Nie, Z.-Y., Li, R.-R., Zhang, W., Wang, H., He, Y.-S., Zhao, L.-J., Li, Y.-X., 2018. Correlation of brain perfusion with white matter hyperintensity, brain atrophy, and cognition in patients with posterior cerebral artery stenosis and subjective cognitive decline. Med. Sci. Monit. 24, 5729.
Marebwa, B.K., Adams, R.J., Magwood, G.S., Basilakos, A., Mueller, M., Rorden, C., Fridriksson, J., Bonilha, L., 2018. Cardiovascular risk factors and brain health: impact on long-range cortical connections and cognitive performance. J. Am. Heart Assoc. 7 (23), e010054.
Misiak, B., Leszek, J., Kiejna, A., 2012. Metabolic syndrome, mild cognitive impairment and Alzheimer's disease—The emerging role of systemic low-grade inflammation and adiposity. Brain Res. Bull. 89 (3-4), 144–149.
Musen, G., Jacobson, A.M., Bolo, N.R., Simonson, D.C., Shenton, M.E., McCartney, R.L., Flores, V.L., Hoogenboom, W.S., 2012. Resting-state brain functional connectivity is altered in type 2 diabetes. Diabetes 61 (9), 2375–2379.

Nielsen, J.A., Zielinski, B.A., Fletcher, P.T., Alexander, A.L., Lange, N., Bigler, E.D., Lainhart, J.E., Anderson, J.S., 2014. Abnormal lateralization of functional connectivity between language and default mode regions in autism. Mol. Autism 5 (1), 8.

Panza, F., Frisardi, V., Seripa, D., P, Imbimbo, B., Sancarlo, D., D'Onofrio, G., Addante, F., Paris, F., Pilotto, A., Solfrizzi, V., 2011. Metabolic syndrome, mild cognitive impairment and dementia. Curr Alzheimer Res. 8 (5), 492–509.

Park, B.-y, Lee, M.J., Kim, M., Kim, S.-H., Park, H., 2018. Structural and functional brain connectivity changes between people with abdominal and non-abdominal obesity and their association with behaviors of eating disorders. Front. Neurosci. 12, 12.

Raffaitin, C., Gin, H., Empana, J.-P., Helmer, C., Berr, C., Tzourio, C., Portet, F., Dartigues, J.-F., Alpérovitch, A., Barberger-Gateau, P., 2009. Metabolic syndrome and risk for incident Alzheimer's disease or vascular dementia: the Three-City Study. Diabetes Care. 32 (1), 169–174.

Rashid, B., Dev, S.I., Esterman, M., Schwarz, N.F., Ferland, T., Fortenbaugh, F.C., Milberg, W.P., McGlinchey, R.E., Salat, D.H., Leritz, E.C., 2019. Aberrant patterns of default-mode network functional connectivity associated with metabolic syndrome: A resting-state study. Brain Behav. 9 (12), e01333.

Reuter-Lorenz, P.A., Jonides, J., Smith, E.E., Hartley, A., Miller, A., Marshuetz, C., Koeppe, R.A., 2000. Age differences in the frontal lateralization of verbal and spatial working memory revealed by PET. J. Cogn. Neurosci. 12 (1), 174–187.

Sala, M., de Roos, A., van den Berg, A., Altmann-Schneider, I., Slagboom, P.E., Westendorp, R.G., van Buchem, M.A., de Craen, A.J., van der Grond, J., 2014. Microstructural brain tissue damage in metabolic syndrome. Diabetes Care. 37 (2), 493–500.

Schaefer, A., Quinque, E.M., Kipping, J.A., Arélin, K., Roggenhofer, E., Frisch, S., Villringer, A., Mueller, K., Schroeter, M.L., 2014. Early small vessel disease affects frontoparietal and cerebellar hubs in close correlation with clinical symptoms—a resting-state fMRI study. J Cereb Blood Flow Metab 34 (7), 1091–1095.

Schwarz, N.F., Nordstrom, L.K., Pagen, L.H., Palombo, D.J., Salat, D.H., Milberg, W.P., McGlinchey, R.E., Leritz, E.C., 2018. Differential associations of metabolic risk factors on cortical thickness in metabolic syndrome. Neuroimage 17, 98–108.

Shin, D., Kongpakpaisarn, K., Bohra, C., 2018. Trends in the prevalence of metabolic syndrome and its components in the United States 2007–2014. Int. J. Cardiol. 259, 216–219.

Singh, V., Chertkow, H., Lerch, J.P., Evans, A.C., Dorr, A.E., Kabani, N.J., 2006. Spatial patterns of cortical thinning in mild cognitive impairment and Alzheimer's disease. Brain 129 (11), 2885–2893.

Solfrizzi, V., Scafato, E., Capurso, C., D'Introno, A., Colacicco, A.M., Frisardi, V., Vendemiale, G., Baldereschi, M., Crepaldi, G., Di Carlo, A, 2011. Metabolic syndrome, mild cognitive impairment, and progression to dementia. The Italian Longitudinal Study on Aging. Neurobiol. Aging 32 (11), 1932–1941.

Sorg, C., Riedl, V., Perneczky, R., Kurz, A., Wohlschlager, A.M., 2009. Impact of Alzheimer's disease on the functional connectivity of spontaneous brain activity. Curr Alzheimer Res. 6 (6), 541–553.

Sun, Y.-w., Zhou, Y., Xu, Q., Qian, L.-j., Tao, J., Xu, J.-r., 2011. Abnormal functional connectivity in patients with vascular cognitive impairment, no dementia: a resting-state functional magnetic resonance imaging study. Behav. Brain Res. 223 (2), 388–394.

Thomas Yeo, B., Krienen, F.M., Sepulcre, J., Sabuncu, M.R., Lashkari, D., Hollinshead, M., Roffman, J.L., Smoller, J.W., Zöllei, L., Polimeni, J.R., 2011. The organization of the human cerebral cortex estimated by intrinsic functional connectivity. J. Neurophysiol. 106 (3), 1125–1165.

Van den Berg, E., Biessels, G., De Craen, A., Gussekloo, J., Westendorp, R., 2007. The metabolic syndrome is associated with decelerated cognitive decline in the oldest old. Neurology 69 (10), 979–985.

Vincent, C., Hall, P.A., 2015. Executive function in adults with type 2 diabetes: a meta-analytic review. Psychosom. Med. 77 (6), 631–642.

Wendell, C.R., Waldstein, S.R., Zonderman, A.B., 2014. Nonlinear longitudinal trajectories of cholesterol and neuropsychological function. Neuropsychology 28 (1), 106.

Wooten, T., Ferland, T., Poole, V., Milberg, W., McGlinchey, R., DeGutis, J., Esterman, M., Leritz, E., 2019. Metabolic risk in older adults is associated with impaired sustained attention. Neuropsychology 33 (7), 947–955.

Xia, W., Wang, S., Rao, H., Spaeth, A.M., Wang, P., Yang, Y., Huang, R., Cai, R., Sun, H., 2015a. Disrupted resting-state attentional networks in T2DM patients. Sci. Rep. 5, 11148.

Xia, W., Zhang, B., Yang, Y., Wang, P., Yang, Y., Wang, S., 2015b. Poorly controlled cholesterol is associated with cognitive impairment in T2DM: a resting-state fMRI study. Lipids Health Dis. 14 (1), 47.

Yaffe, K., Kanaya, A., Lindquist, K., Simonsick, E.M., Harris, T., Shorr, R.I., Tylavsky, F.A., Newman, A.B., 2004. The metabolic syndrome, inflammation, and risk of cognitive decline. JAMA 292 (18), 2237–2242.

Yaffe, K., Weston, A.L., Blackwell, T., Krueger, K.A., 2009. The metabolic syndrome and development of cognitive impairment among older women. Arch. Neurol. 66 (3), 324–328.

Yates, K.F., Sweat, V., Yau, P.L., Turchiano, M.M., Convit, A., 2012. Impact of metabolic syndrome on cognition and brain: a selected review of the literature. Arterioscler. Thromb. Vasc. Biol. 32 (9), 2060–2067.